14TH CANADIAN MASONRY SYMPOSIUM
MONTREAL, CANADA
MAY 16TH – MAY 20TH, 2021

EXPERIMENTAL ASSESSMENT OF THE SEISMIC PERFORMANCE OF CONTROLLED ROCKING MASONRY WALLS WITHOUT POST-TENSIONING

Yassin, Ahmed[1]; Ezzeldin, Mohamed[2] and Wiebe, Lydell[3]

ABSTRACT

In recent years, several studies have been conducted to evaluate the seismic response of controlled rocking reinforced masonry walls with unbonded post-tensioning (PT) tendons. This system is considered appealing because of the low damage associated with these walls due to their self-centring capability following a seismic event. However, several challenges associated with post-tensioning in masonry construction practice still exist. These include the relatively high prestressing losses and the increased demands at the wall compression toes. Such challenges clearly demonstrate the importance of considering an alternative source of self-centring. In this respect, this paper reports the results from a series of experimental tests that were conducted on two Energy Dissipation-Controlled Rocking Masonry Walls (ED-CRMWs) to evaluate the capability of the system to self-centre through vertical gravity loads only, without the use of PT tendons. Both walls were half-scale concrete masonry blocks and fully grouted, with identical dimensions and amounts of energy dissipation. However, one wall was without any confinement, while the other wall had end confined boundary elements using closed ties. The two walls were tested under quasi-static loading with fully-reversed cycles up to failure. The current study focuses first on the ability of the system to dissipate energy while preserving the advantage of localized damage. The study then explores the influence of toe confinement using boundary elements in enhancing the seismic response of ED-CRMWs. The experimental results are discussed with respect to the observed damage, residual drifts, and displacement ductility capacities.

KEYWORDS: *self-centering, controlled rocking, experimental testing, energy dissipation*

[1] Ph.D. Candidate, Department of Civil Engineering, McMaster University, 1280 Main St W, Hamilton, ON, Canada yassia1@mcmaster.ca
[2] Assistant Professor, Department of Civil Engineering, McMaster University, 1280 Main St W, Hamilton, ON, Canada, ezzeldms@mcmaster.ca
[3] Associate Professor, Department of Civil Engineering, McMaster University, 1280 Main St W, Hamilton, ON, Canada, wiebel@mcmaster.ca

INTRODUCTION

Conventional fixed walls (i.e., special reinforced masonry walls, SRMWs) are designed for a reduced lateral force, which comes at the expense of accepting damage in potential plastic hinge zones that are specifically detailed for ductility. However, significant damage associated with large residual lateral displacements and wide residual cracks is expected to occur with such systems. Consequently, such a design approach does not account for the costs associated with the loss of operation and service shutdown that would be required for structural restoration and rehabilitation following moderate to strong earthquakes. This process hinders the overall resilience of such systems. On the other hand, controlled rocking walls are considered an appealing alternative to overcome the main disadvantages of conventional fixed walls.

Controlled rocking wall systems with vertical unbonded post-tensioning gained attention through the Precast Seismic Structural Systems (PRESSS) project [1, 2] using reinforced precast concrete shear walls. The main experimental observations and results of PRESSS showed that the damage was limited and concentrated at the wall toes with a single crack at the wall-foundation rocking interface. In addition, controlled rocking walls achieved a desirable self-centring response, with almost zero residual drift at the end of the experimental test. Moreover, the lateral response of controlled rocking walls was governed mainly by rocking deformations, while the flexural and shear deformations were minimal [3]. These promising results led researchers to perform further investigations in an effort to enhance the seismic performance of this system [4, 5, 6] and to explore the potential of using masonry walls instead of concrete counterparts [7, 8, 9].

The first study of controlled rocking masonry walls with unbonded post-tensioning (PT-CRMWs) was reported by Laursen [10], where six fully-grouted walls, one partially-grouted and one ungrouted wall were tested in the first phase using concrete masonry units. The experimental results demonstrated that the behaviour of fully-grouted walls was similar to that of precast concrete walls regarding self-centring ability and localization of damage at the wall base. Similarly, Rosenboom and Kowalsky [11] conducted experimental tests on five controlled rocking walls using clay masonry blocks instead of concrete blocks. The study investigated the effects of bonded and unbonded post-tensioning (PT) bars, as well as the effect of supplemental mild steel and confinement plates on the behaviour of PT-CRMWs. Recently, Hassanli et al. [12] tested four fully-grouted concrete masonry walls with different initial prestressing to yielding stress ratio and different distributions of unbonded post-tensioned bars. A study on the seismic collapse risk of PT-CRMWs has also been conducted [13].

Although such a system (i.e, PT-CRMW) is considered promising because of the low damage associated with the wall and its ability to self-centre, the problem of PT losses, the difficulty of implementation during construction, and inspection following a seismic event continue to be challenging. This situation leads to a motivation to experimentally investigate an alternative source to control wall rocking. In this respect, using a new controlled rocking technique, the current study describes the experimental testing of two reinforced fully-grouted masonry shear walls under displacement-controlled cyclic loading. Specifically, the tested CRMWs had no post-tensioning

(PT) tendons; instead, the walls were designed such that axial load from the tributary floor area provides self-centring ability to the system. In addition, to control lateral displacements and increase system damping, an energy dissipation (ED) device was introduced, resulting in an ED-controlled rocking masonry wall (ED-CRMW). The first objective of this study is to evaluate the ability of the proposed system to self-centre with minimum residual drifts and to also localize the damage at the wall toes only, as an alternative to PT-CRMW counterparts. Figures 1a and 1b schematically show the characteristic lateral response of SRMWs (full hysteresis) and ED-CRMWs (flag-shaped hysteresis).

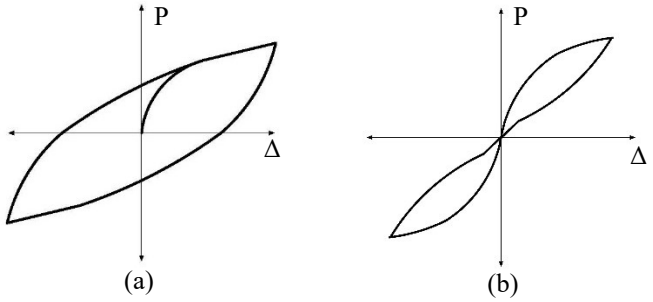

Figure 1: Lateral response of a) SRMWs and b) ED-CRMWs

The second objective of this study is to investigate the effect of using end-confined boundary elements using closed ties. This technique has been implemented in SRMWs by many researchers (Shedid et al. [14], Banting and El-Dakhakhni [15], Ezzeldin et al. [16]); however, it has not been applied before to a controlled rocking masonry wall. Thus, the level of enhancement achieved by implementing end-confined boundary elements using pilaster units is experimentally reported in the current study.

TEST MATRIX

The experimental program consisted of two two-storey half-scale walls that were designed to have a similar ultimate resistance in order to directly compare their seismic performance. The half-scale concrete masonry blocks employed in this study are true replicas of the full-scale 200 mm concrete blocks widely used in North America. Each wall has a length of 1895 mm, a height of 2660 mm, and a thickness of 90 mm, resulting in an aspect ratio of 1.4 for both walls. The two-storey walls had a reinforced concrete slab constructed at each storey level to capture their effects on the cracking pattern of the rocking walls.

The test matrix is summarized in Table 1. The rectangular wall, W1, was constructed using ten blocks along the web, while the end boundary wall, W2, was constructed using eight blocks along the web and two pilaster units (185 mm x 185 mm) placed at the end of the web. The elevation and the side view of the two walls are shown in Figure 2, illustrating the overall dimensions of the wall in addition to its storey slabs and foundation.

Table 1: Experimental walls test matrix

Specimen	Wall Type	Wall Dimension	Vertical Reinforcement	Horizontal Reinforcement	Confinement
W1	Rectangular	1895 mm x 2660 mm (length x height)	6D7 + 2M10	D4 every other course	N.A.
W2	End Boundary		4D7 + 2M10 @ Web 8D7 @ End Boundary		D4 closed ties every other course

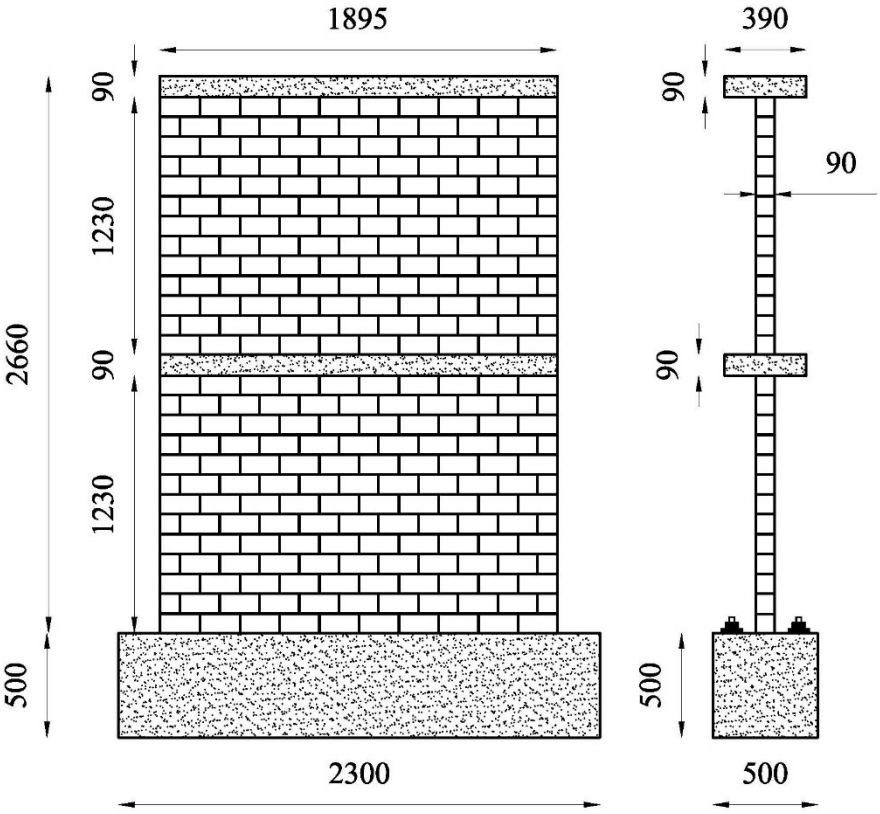

Figure 2: Wall dimensions in elevation and side view

Minimum bonded vertical reinforcement was used in the two walls according to the CSA S304-14 [17], and all bonded reinforcement was not connected or embedded to the foundation but terminated at the wall-foundation interface. These vertical bonded bars were used in order to maintain wall integrity during rocking and to satisfy the requirement of the design standard for seismic detailing. D7 bars (area = 50 mm^2) were used as the bonded vertical reinforcement for both walls; however, since these bars were not extended to the foundation, they did not contribute to wall strength.

The energy dissipation used in both walls was two M10 (area = 100 mm^2) unbonded bars with an unbonded length, L_{un}, of 900 mm, anchored to a steel plate at -400 mm below the wall-foundation interface, unbonded up to +500 mm above the wall-foundation interface, and bonded from that elevation until the top slab level (+2660 mm), as shown in Figure 3. A PVC tube was used to ensure no grout reached the M10 energy dissipation bar along the unbonded length, L_{un}.

Both walls were subjected to an axial load of 200 kN that was held constant throughout the test and was applied at the top of the wall by two hydraulic jacks. This axial load represents the tributary area gravity load, which corresponds to $6.5\%A_g f'_m$.

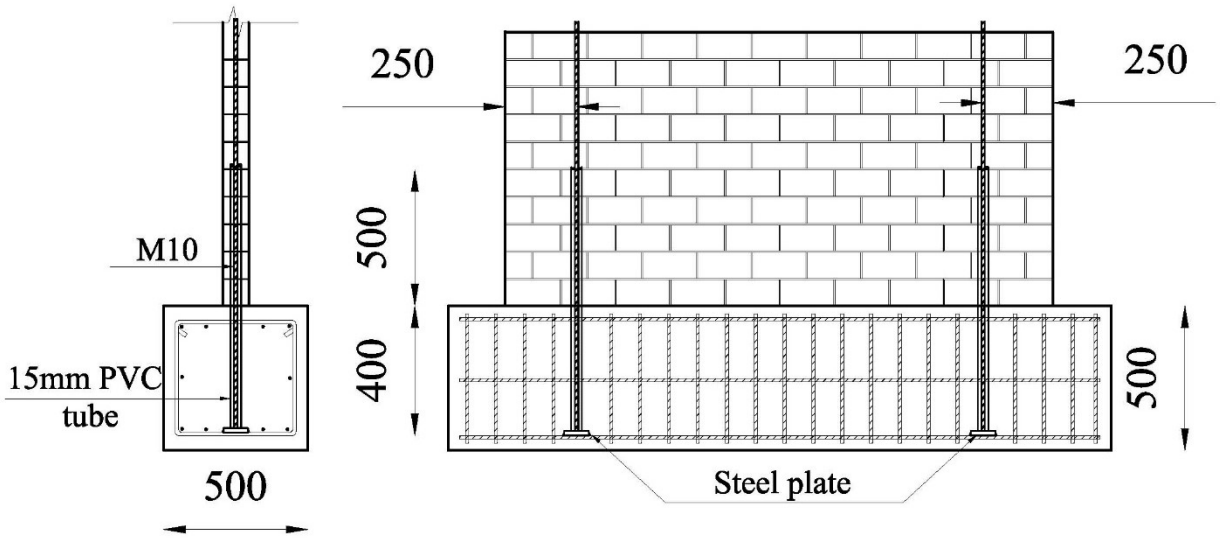

Figure 3: Unbonded length detailing for the energy dissipation

Three masonry prisms, each four blocks high by one block long (375 mm high x 185 mm long x 90 mm thick), were constructed and grouted during each construction stage, resulting in a total of 24 prisms. These prisms were tested to determine the masonry compressive strength. The average compressive strength of the grouted masonry prisms, f'_m, was 18.9 MPa with a COV = 14.2%. Tension tests were also conducted on the M10 energy dissipation bars. The average yield strength of the bars was 476 MPa with a COV = 4.2% and the average Young's modulus of 200.5 GPa with a COV = 2.1%.

EXPERIMENTAL RESULTS

The test results including failure modes and the extent of wall damage are presented in this section, as shown in Figure 4. Also, the cyclic response of both walls is discussed based on the hysteresis loops, as presented in Figure 5. In the current study, the FEMA 461 [18] quasi-static testing protocol was adopted.

Failure Modes and Extent of Damage

Generally, each wall showed a pure rocking response characterized by a gap opening at the rocking interface joint between the wall and its foundation. No evidence of any other flexural tension cracks was observed during the test. At later stages of loading (2.5% drift), a superficial diagonal tension shear crack was observed in wall W1, whereas no shear cracks were observed in wall W2 throughout the test. No sliding was observed between the wall and the foundation until the end of the test with the use of stoppers at wall ends. The damage to both walls is shown in Figure 4.

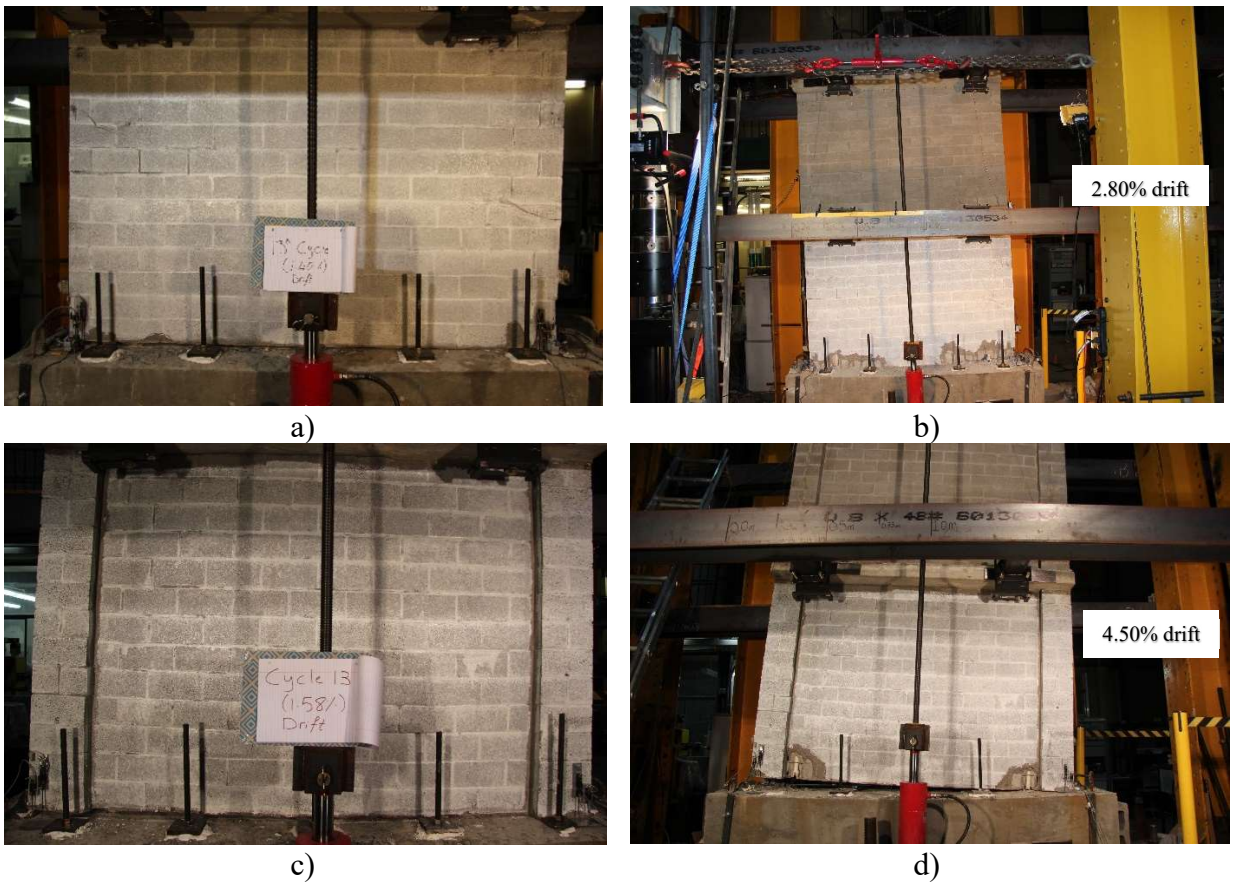

a) b)

c) d)

Figure 4: Damage of walls at a) 1.46% drift for W1, b) the end of test for W1 @ 2.80% drift, c) 1.58% drift for W2, and d) the end of test for W2 @ 4.50% drift

Gap opening at the base rocking interface started at drift ratios of 0.08% and 0.10% for walls W1 and W2, respectively. Afterward, the energy dissipation for both walls began to yield at 0.21% drift. The initiation of a partial face shell spalling at crushing toes was observed at 0.60% for wall W1 and 0.70% for wall W2. Minor vertical splitting cracks were observed at the wall toes at drift ratios of 1.54% and 2.00% for walls W1 and W2, respectively. Afterward, a distinctive behaviour of each wall was observed, as described below.

For rectangular wall W1, vertical cracks and crushing of the rocking toe were observed at a drift ratio of 1.70% along the full-block height of the bottommost block, followed by propagation of face shell spalling and eventually crushing for the inward blocks of the first course, leading to

strength degradation in the wall response until a drift ratio of 2.80%, which corresponded to 50% strength degradation.

For end boundary wall W2, due to the presence of closed stirrups at the pilaster blocks, the vertical cracks of the rocking toe were confined, thus the confined core which was subjected to high compression demands did not deteriorate. Therefore, no strength degradation or progression of damage was observed up to 2.40% drift. Afterward, the pronounced uplift elongation and low cyclic fatigue in the ED bars caused a fracture of both bars (i.e., at push and pull directions), leading to a sudden reduction in the wall strength by approximately 30%, which corresponds to the designed contribution of energy dissipation, while 70% of the wall strength was retained because of the axial load. The test continued until 4.90% drift, where the wall responded in a free rocking mode with essentially no energy dissipated, as shown in Figure 5. Although the wall did not reach 50% strength degradation, the test was terminated at this drift ratio because the maximum stroke of the actuator was reached.

Force-Displacement Response

The force measured during the experiments, using the actuator load cell, and the corresponding lateral displacement measured at the middle of the loading beam for each wall, are presented in Figure 5. In general, stable hysteretic loops were observed in the cyclic response for walls W1 and W2. For the rectangular wall (W1), the peak strength was 95 kN and 94.5 kN in the push and pull directions, respectively, at a drift of 1.55%, while the end boundary wall (W2) reached peak strengths of 103 kN and 103.5 kN in the push and pull directions, respectively, at a drift of 2.40%.

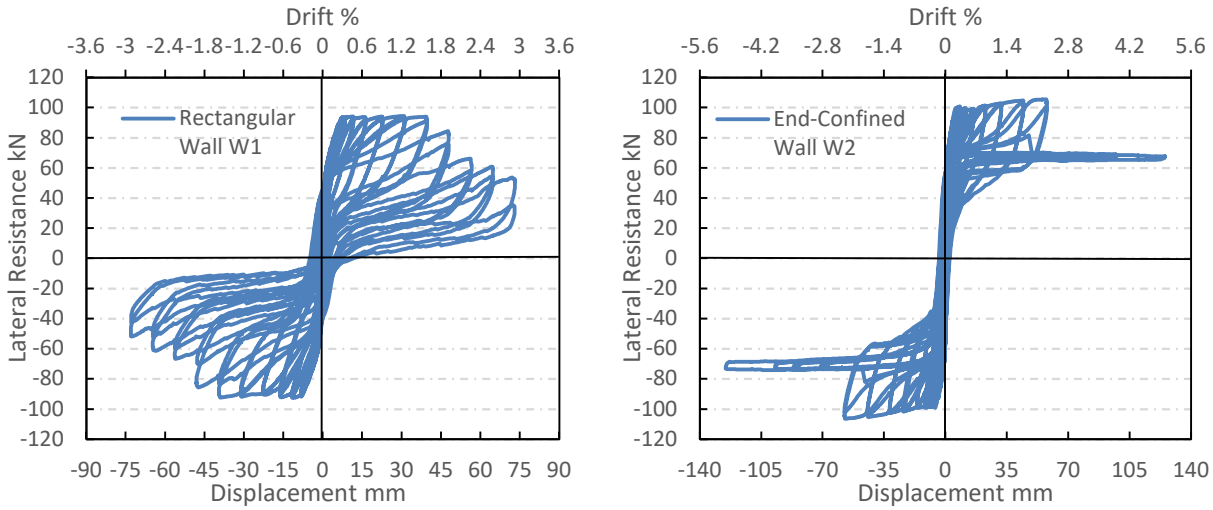

Figure 5: Hysteresis loops for walls W1 and W2

As shown in Figure 5, wall W1 experienced gradual strength degradation due to deterioration of the rocking toe, reaching 80% of its ultimate strength at a drift ratio of 2.00%. For wall W2, no strength degradation due to rocking toe crushing was observed; however, due to the symmetrical fracture of both energy dissipation bars, a sudden 30% loss of strength of the ultimate strength took place at 2.40% drift in both push and pull directions.

Compression Zone Depth Variation

To track the compression zone depth variation during the test, five string potentiometers were attached along the wall–foundation interface. As shown in Figure 6, the rocking joint gap opening widens as the drift ratio increases. For example, for the rectangular wall W1, at a drift ratio of 2.75%, the wall gap opening reached approximately 31.6 mm at the extreme left sensor.

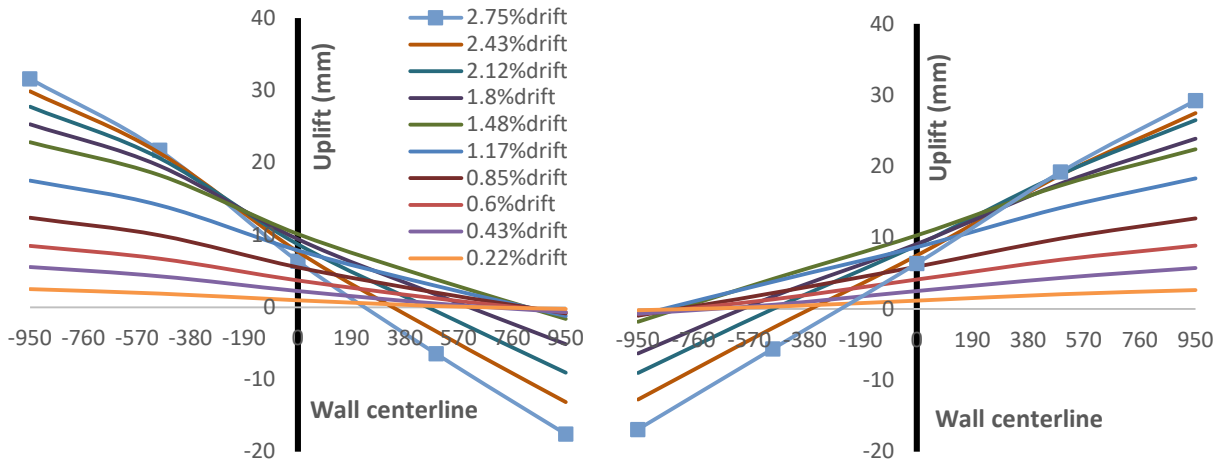

Figure 6: Base crack profile for rectangular wall W1

Figure 7 shows the compression zone depth variation at different drift levels. As shown in Figure 7, for rectangular wall W1, the compression zone depth, c, normalized to the wall length, L_w, decreased steeply until approximately 0.25% drift, after which the compression zone depth, c, stabilized at approximately 9% of the wall length, which corresponds to 130 mm and agrees well with the design value. Afterward, the crushing of the compression toe led to inward shifting of the neutral axis depth, leading to an increase of the compression zone depth. For the end confined wall W2, due to the preservation of the compression zone without significant deterioration, the compression zone length, c, was consistent at a small value of 3% of wall length due to the enlarged boundary width.

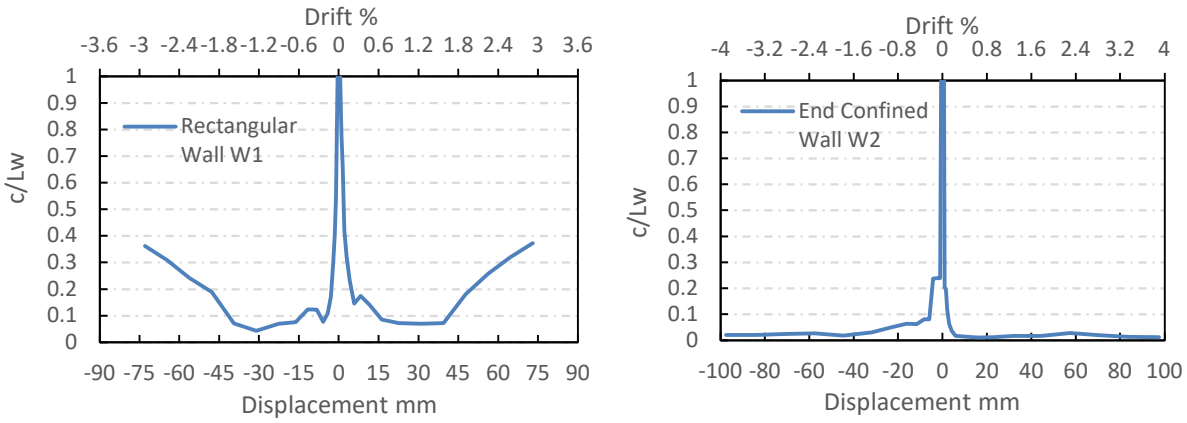

Figure 7: Compression zone depth variation with drift

Self-Centring Capability

To ensure self-centering of the system, the ratio between the moment contribution due to ED to the moment contribution due to restoring forces (i.e., gravity load) must be less than unity. In this study, the walls were designed such that this ratio was 0.35. At the end of the first cycle at each displacement level, the lateral drift at the point of zero lateral force was considered as the residual drift (d_r), and was used to quantify the self-centring capability of the tested ED-CRMWs. In Figure 8, the residual drift, d_r, in the imposed cycle is plotted against the corresponding drift of the same cycle. As shown in the figure, the residual drifts for end-confined wall W2 remained limited to 0.1% until the end of the test. However, the rectangular Wall W1 exhibited an increased residual drift reaching a maximum of 0.43% at the end of the test due to significant crushing of rocking toes. This illustrates the advantage of using confined end boundary elements, which protect rocking toes from deterioration and maintain self-centring capability throughout the test. In general, the ED-CRMWs can achieve similar behaviour as PT-CRMWs regarding self-centring capability, even with the yielding of energy dissipation bars and without the use of PT.

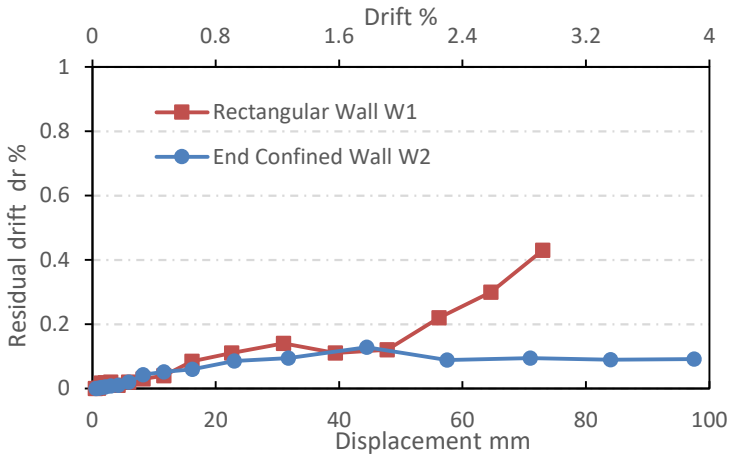

Figure 8: Residual drifts for wall W1 and W2

Displacement Ductility

Displacement ductility, μ_{Δ}, is used to evaluate and compare the post-peak behaviour of the rectangular (W1) and end confined (W2) ED-CRMWs. The displacement ductility, $\mu_{\Delta 0.8u}$, is defined as the ratio between the displacement corresponding to degradation to 80% of the strength and the displacement corresponding to the onset of the energy dissipation bar yielding without any idealization of the load-displacement relationship. The displacement for the onset of energy dissipation bar yielding, Δ_y, was 4.2 mm for both walls. However, the displacement corresponding to degradation to 80% of the strength, $\Delta_{0.8u}$, was 47 mm and 59 mm for walls W1 and W2, respectively. Thus, the displacement ductility, $\mu_{\Delta 0.8u}$, is 11.2 and 14.4 for rectangular and end confined walls, respectively. This reflects the enhancement due to confining the end boundary, given the fact that the strength degradation is not due to masonry crushing but due to energy dissipation fracture, which would be avoided if a longer unbonded length was used, thus achieving higher ductility.

CONCLUSIONS

The performance of two ED-CRMWs with different end configurations was investigated. Both rectangular (W1) and end-confined (W2) shear walls were tested under displacement-controlled quasistatic cyclic loading. The response of the tested walls showed a symmetrical loading response in both directions with stable hysteresis loops, which increased due to progressive yielding of the energy dissipation bars.

The test results of these ED-CRMWs demonstrated that relying on gravity loads from slabs still maintained the high performance of the rocking wall regarding the self-centring capability (0.1% residual drift), the localized damage, and the high drift capacity. In addition, considering the cost savings by avoiding the post-tensioning process and with the simplicity of the energy dissipation used, ED-CRMWs are an appealing alternative to PT-CRMWs.

The effect of closed ties as a confining technique in end confined boundaries significantly enhanced the performance of wall W2 compared to the rectangular wall W1, given that the sudden drop in strength was only due to the energy dissipation fracture and could thus be delayed through different detailing of the energy dissipation. This was demonstrated through the reduced extent of damage that was observed at the crushing toes, with only superficial vertical cracks on the face shell while the confined core remained intact. This was also reflected by the self-centring capability, where the end confined wall achieved a residual drift of only 0.1% only for a drift ratio of 3.9%.

ACKNOWLEDGEMENTS

The financial support for this project was provided through the Canadian Concrete Masonry Producers Association (CCMPA), the Canada Masonry Design Centre (CMDC), the Natural Sciences and Engineering Research Council (NSERC) and the Ontario Centres of Excellence (OCE).

REFERENCES

[1] Priestley, M. J. N., Sritharan, S., Conley, J. R., and Pampanin, S. (1999). “Preliminary results and conclusions from the PRESSS five-story precast concrete test building.” *PCI Journal*, 44(6), 42-67.

[2] Schultz, A. E. and Magana, R. A. (1998). “Performance of precast concrete shear walls.” *6th U.S. National Conference on Earthquake Engineering*. Earthquake Engineering Research Institute.

[3] Nakaki, S. D., Stanton, J. F., and Sritharan, S. (1999). “An overview of the PRESSS five-story precast concrete test building.” *PCI Journal*, 44(2), 26–39.

[4] Henry, R. S., Brooke, N. J., Sritharan, S., and Ingham, J. M. (2012). “Defining concrete compressive strain in unbonded post-tensioned walls.” *ACI Journal*, 109(1), 101-112.

[5] Holden, T., Restrepo, J., Mander, J. B. (2003). “Seismic performance of precast reinforced and prestressed concrete walls.” *J. Struct. Eng.*, 129(3), 286-296.

[6] Kurama, Y., Pessiki, S., Sause, R., and Lu, L. W. (1999). “Seismic behavior and design of unbonded post-tensioned precast concrete walls.” *PCI Journal*, 44(3), 72-89.

[7] Laursen, P. T. and Ingham, J. M. (2001). "Structural Testing of Single-Storey Post-Tensioned Concrete Masonry Walls." *The Professional Journal of The Masonry Society*, 19(1), 69-82.
[8] Laursen, P. T. and Ingham, J. M. (2004). "Structural testing of enhanced post-tensioned concrete masonry walls." *ACI Journal*, 101(6), 852-862.
[9] Laursen, P. T. and Ingham, J. M. (2004). "Structural testing of large-scale posttensioned concrete masonry walls." *J. Struct. Eng.*, 130(10), 1497-1505.
[10] Laursen, P. T. (2002). "Seismic analysis and design of post-tensioned concrete masonry walls." PhD Thesis, Department of Civil and Environmental Engineering, University of Auckland.
[11] Rosenboom, O. A. and Kowalsky, M. J. (2004). "Reversed in-plane cyclic behavior of posttensioned clay brick masonry walls." *J. Struct. Eng.*, 130(5), 787–798.
[12] Hassanli, R., ElGawady, M., and Mills, J. (2016). "Experimental investigation of in-plane cyclic response of unbonded-posttensioned masonry walls." *J. Struct. Eng.*, 142(5), 04015171-1-15.
[13] Yassin, A., Ezzeldin, M., Steele, T., and Wiebe, L. (2020). "Seismic collapse risk assessment of post-tensioned controlled rocking masonry walls." *J. Struct. Eng.*, 146(5), 04020060-1-16.
[14] Shedid, M., El-Dakhakhni, W., and Drysdale, R. (2010). "Alternative Strategies to Enhance the Seismic Performance of Reinforced Concrete-Block Shear Wall Systems." *J. Struct. Eng.*, 136(6), 676–689.
[15] Banting, B. R. and El-Dakhakhni, W. W. (2012). "Force- and displacement-based seismic performance parameters for reinforced masonry structural walls with boundary elements." *J. Struct. Eng.*, 138(12), 1477-1491.
[16] Ezzeldin, M., El-Dakhakhni, W., and Wiebe, L. (2017). "Experimental assessment of the system-level seismic performance of an asymmetrical reinforced concrete block–wall building with boundary elements." *J. Struct. Eng.*, 143(8), 04017063.
[17] CSA (Canadian Standards Association). (2014). "Design of Masonry Structures." *CSA S304.1-14*, Mississauga, ON.
[18] FEMA. (2007). "Interim testing protocols for determining the seismic performance characteristics of structural and nonstructural components." *FEMA 461*, Washington, DC.